Conjugated Conduction-Free Convection Heat Transfer in an Annulus Heated at Either Constant Wall Temperature or Constant Heat Flux

HAROON IMTIAZ*, AND FATHI MOHAMAD MAHFOUZ**

RECEIVED ON 13.09.2015 ACCEPTED ON 11.05.2016

ABSTRACT

In this paper, we investigate numerically the effect of thermal boundary conditions on conjugated conduction-free convection heat transfer in an annulus between two concentric cylinders using Fourier Spectral method. The inner wall of the annulus is heated and maintained at either CWT (Constant Wall Temperature) or CHF (Constant Heat Flux), while the outer wall is maintained at constant temperature. CHF case is relatively more significant for high pressure industrial applications, but it has not received much attention. This study particularly focuses the latter case (CHF). The main influencing parameters on flow and thermal fields within the annulus are: Rayleigh number Ra; thickness of inner wall Rs; radius ratio Rr and inner wall-fluid thermal conductivity ratio Kr. The study has shown that the increase in Kr increases the heat transfer rate through the annulus for heating at CWT and decreases the inner wall dimensionless temperature for heating at CHF and vice versa. It has also been proved that as the Rs increases at fixed Ra and Rr, the heat transfer rate decreases for heating at CWT and the inner wall dimensionless temperature increases for heating at CHF at Kr <1. The study has also discussed that the effect of increase in Rs for both cases of heating at Kr>1 depends on Rr. It has been shown that for certain combinations of controlling parameters there will be a value of Rr at which heat transfer rate will be minimum in the annulus in case of heating at CWT, while there will be a value of Rr at which inner wall dimensionless temperature will be maximum in case of heating at CHF.

Key Words: Fourier Spectral Method, Finite Difference Method, Free Convection, Conjugate Heat Transfer, Concentric Annulus.

1. INTRODUCTION

Buoyancy driven flow and associated heat transfer in an annular enclosure between two concentric/eccentric circular walls has long been investigated because of its pertinence to many practical engineering applications. These applications include thermal storage systems, solar collector-receivers, underground power transmission cables, cooling system in nuclear reactor and many others [1]. The heat transfer in such geometry occurs as a result of temperature difference created due to heating of one wall and cooling

* Department of Mechanical Engineering, College of Electrical & Mechanical Engineering, National University of Sciences & Technology, Islamabad.
** Department of Mechanical Power, Menoufia University, Egypt.

the other. The heating process may be done at either prescribed wall temperature or prescribed heat flux. The present work considers heating the inner wall at either CWT or CHF while outer wall is cooled and maintained at constant temperature. The case of isothermal heating (CWT) approximates the cooling of microelectronic equipment while dissipation of heat generated within an underground power transmission cables from its surface to the surrounding enclosure is a practical example of heating at CHF [2].

Buoyancy driven flows within annular enclosures have been studied both numerically and experimentally by a number of authors [3-26]. These previous studies may be categorized based on heating at CWT [3-21] or at CHF [22-26]. In case of CWT the most early and reliable experimental and numerical work on natural convection within concentric annulus containing air or water was done by Kuehn and Goldstein [3], who used Mach-Zehnder interferometer to conduct the experimental study and performed numerical investigation using finite difference method. Since then, CWT case has been further examined by a number of researchers [4-21] who conducted experimental and theoretical works not only to investigate the effect of different controlling parameters such as Prandtl number and different geometry configurations on heat convection within such annuli, but also to verify various numerical and experimental techniques.

In case of CHF heating, only a few studies were reported for natural convection within concentric annulus [22-26]. Kumar [22] showed that wall temperature is a function of diameter ratio and Rayleigh number. On the other hand, Castrejon and Spalding [23] made an experimental and theoretical study of transient free-convective flow between horizontal concentric cylinders. Yoo [24] discussed flow pattern of natural convection while Yoo [25] studied dual free-convective flows in a horizontal annulus with constant heat flux on inner wall. Ho, et. al. [26] conducted a numerical study of natural convection in concentric and eccentric horizontal cylindrical annuli with mixed boundary conditions.

The thermal boundary conditions definitely affect the flow and thermal fields within the concentric annulus. A common practice adopted by heat transfer community, as can be inferred from previous works [3-26], is to prescribe thermal boundary condition at the fluid-wall interface. Consequently, energy equation of fluid alone has to be solved and numerical results become unreliable for wall having high thickness or low thermal conductivity. In most of high-pressure industrial applications, thickness of wall is high and conduction in solid wall needs to be coupled with convective heat transfer in fluid (named as conjugate heat transfer).

The effect of conjugation for Newtonian fluid in a concentric annulus was considered by Kolesnikov and Bubnovich [27]. The authors investigated conjugated conduction-free-convective heat transfer in horizontal cylindrical coaxial channels subjected to CWT heating. The case of CHF heating is more relevant to industrial applications than CWT case but it has not been widely investigated so far as per author's best knowledge. The objective of this study is to investigate conjugate heat transfer through concentric annulus, heated either isothermally or through constant heat flux with focus on the latter case (CHF). Moreover, the study aims to provide accurate numerical results by adopting numerical solution based on Fourier Spectral method.

2. PROBLEM FORMULATION AND SOLUTION

Fig. 1 illustrates the physical domain of the problem which is the annulus space between two long concentric cylinders. The inner cylinder has inner radius r_i (heating side) and outer radius r_{sf} (fluid side), while outer wall has radius r_o. The

fluid media is assumed to be Newtonian, Fourier and incompressible. Newtonian implies that the stress tensor is linearly related to rate of strain tensor. Fourier fluid is the one for which conduction part of the fluid is linearly related to the temperature gradient. The inner cylinder is impulsively heated from its inner side either at constant temperature T_i or through constant heat flux q_i. The temperature of outer cylinder is cooled and maintained at constant low temperature T_o. The resulting buoyancy driven flow between concentric cylinders is assumed two dimensional and laminar. The density of fluid is constant excluding the buoyancy term where it varies according to Buossinesq approximation.

2.1 The Governing Equations

For Buoyancy driven flow, time dependent governing equations of mass, momentum and energy in Cartesian coordinates in terms of stream function, vorticity and temperature for the above mentioned problem can be written as:

$$\frac{\partial \xi'}{\partial \tau}+\frac{\partial \psi'}{\partial y}\frac{\partial \xi'}{\partial x}-\frac{\partial \psi'}{\partial x}\frac{\partial \xi'}{\partial y}=\upsilon\nabla^2\xi'-\frac{1}{\rho}\frac{\partial F_x}{\partial y} \tag{1}$$

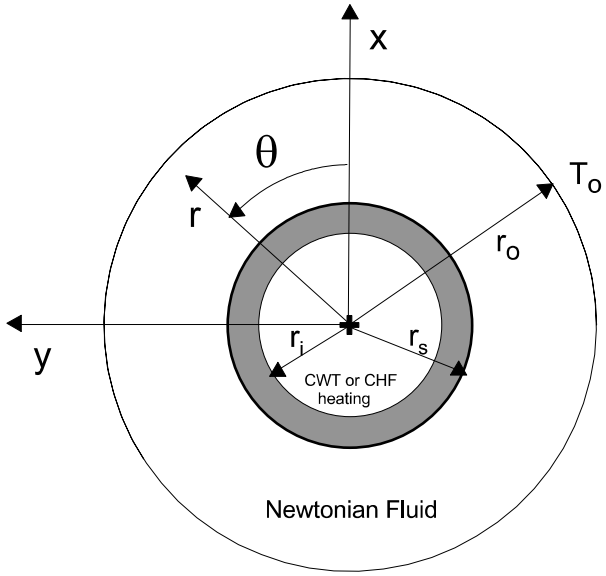

FIG. 1. GEOMETRY OF THE PROBLEM TEMPERATURE AT OUTER WALL T_o, CARTESIAN COORDINATES (X,Y) AND POLAR COORDINATES (r.θ)

$$\xi' = \nabla^2\psi' \tag{2}$$

Energy equation in fluid part ($r_{sf} \le r \le r_o$)

$$\frac{\partial T}{\partial \tau}+\frac{\partial \psi'}{\partial y}\frac{\partial T}{\partial x}-\frac{\partial \psi'}{\partial x}\frac{\partial T}{\partial y}=\alpha\left(\frac{\partial^2 T}{\partial x^2}+\frac{\partial^2 T}{\partial y^2}\right) \tag{3}$$

In the solid wall of the inner cylinder ($r_i \le r \le r_{sf}$) the energy equation can be written as:

$$\frac{\partial T}{\partial \tau}=\alpha_s\left(\frac{\partial^2 T}{dx^2}+\frac{\partial^2 T}{\partial y^2}\right) \tag{4}$$

Where τ is the time, ψ' is the stream function, ζ' is the vorticity, T is the temperature, ρ is the density, v is the kinematic viscosity and $F_x = \rho g\beta\,(T-T_o)$ is upward buoyancy force F_b.k_s, α_s and k_f, α are thermal conductivity and thermal diffusivity of the solid and fluid respectively.

2.2 Initial and Boundary Conditions

Initial conditions are required since the governing equations are time dependent. The inner wall of annulus is heated instantaneously at t = 0 either to CWT T_i or to CHF q_i. The outer wall of concentric annulus is maintained at temperature T_o.

Boundary conditions at inner wall heating side

$$T = T_i \text{ for CWT q} = k_s\frac{\partial T}{\partial s_n} = q_i \text{ for CHF} \tag{5}$$

s_n is the direction of heat flux normal to surface.

Boundary conditions at inner wall fluid side

$$\psi' = \frac{\partial \psi'}{\partial y} = \frac{\partial \psi'}{\partial x} = 0 \tag{6}$$

Boundary conditions at outer wall

$$\psi' = \frac{\partial \psi'}{\partial y} = \frac{\partial \psi'}{\partial x} = 0 \tag{7}$$

$$T = T_o \tag{8}$$

Now introducing the variables

$$t = \frac{\tau\alpha}{r_i^2}, \bar{x} = \frac{x}{r_i}, \bar{y} = \frac{y}{r_i}, R = \frac{r}{r_i}, \psi = \frac{\psi'}{\alpha}, \xi' = -\xi' \frac{r_i^2}{\alpha}, \phi = \frac{T - T_o}{\Delta T_{ref}}$$

And using the modified polar coordinates (ξ, θ) as $\bar{x} = e^{\xi}\cos\theta, \bar{y} = e^{\xi}\sin\theta$, Equations (1-4) can be written as:

$$J\frac{\partial \xi}{\partial t} = pr\left[\frac{\partial^2 \xi}{\partial \xi^2} + \frac{\partial^2 \xi}{\partial \theta^2}\right] + \frac{\partial \psi}{\partial \xi}\frac{\partial \xi}{\partial \theta} - \frac{\partial \xi}{\partial \theta}\frac{\partial \xi}{\partial \xi} + \frac{1}{8}Je^{-\xi}Ra\,\mathrm{Pr}\left[\frac{\partial \phi}{\partial \xi}\sin\theta + \frac{\partial \phi}{\partial \theta}\cos\theta\right] \tag{9}$$

$$J\zeta = \frac{\partial^2 \psi}{\partial \xi} + \frac{\partial^2 \psi}{\partial \theta^2} \tag{10}$$

Energy equation in case of solving in fluid domain

$$J\frac{\partial \phi}{\partial t} = \left[\frac{\partial^2 \phi}{\partial \xi^2} + \frac{\partial^2 \phi}{\partial \theta^2}\right] + \frac{\partial \psi}{d\psi}\frac{\partial \phi}{\partial \theta} - \frac{\partial \psi}{\partial \theta}\frac{\partial \phi}{d\xi} \tag{11}$$

Energy equation in case of solving in solid domain

$$J\frac{\partial \phi}{\partial t} = \frac{\alpha_s}{\alpha}\left[\frac{\partial^2 \phi}{\partial \xi^2} + \frac{\partial^2 \phi}{\partial \theta^2}\right] \tag{12}$$

Where $J=e^{2\xi}$, (ξ= ln R) is the Jacobian of coordinate transformation matrix, Pr = ν/α is the Prandtl number, $Ra=g\beta(2r_i)^3\,\Delta T_{ref}/\nu\alpha$ is the Rayleigh number (called modified Rayleigh number, Ra_F in case of CHF) and ΔT_{ref} is the reference temperature difference and is $= T_i - T_o$ in case of CWT while it is $= q_i\, r_i/k$ in case of CHF. The definition of Rayleigh number ($=g\beta L^2\Delta T_{ref}/\nu\alpha$) was used in the previous works and thus is used in case of comparisons with those works.

These steady boundary conditions in the modified coordinates can be expressed as:

$$\psi = \frac{\partial \psi}{\partial \theta} = 0, \frac{\partial \psi}{\partial \xi} = 0, \text{and } \phi = \text{I for GWT, while } \frac{\partial \phi}{\partial \xi} = \frac{1}{\text{kr}} \text{ for CHF} \tag{13}$$

At inner wall $\xi = \xi_i$

At solid-fluid interface $\xi = \xi_{sf}$

$$\psi = 0,\ e^{-\xi}\frac{\partial \psi}{\partial \theta} = 0,\ e^{-\xi}\frac{\partial \psi}{\partial \xi} = 0, \text{and } k_s \left.\frac{\partial \phi}{\partial \xi}\right|_{solid} = k f \left.\frac{\partial \phi}{\partial \xi}\right|_{fluid} \tag{14}$$

At outer wall $\xi = \xi_o$

$$\psi = \frac{\partial \psi}{\partial \theta} = 0, \frac{\partial \psi}{\partial \xi} = 0, \text{and } \phi = 0 \tag{15}$$

2.3 Method of Solution and Numerical Procedure

The process of solving the governing Equations (9-12) in modified polar coordinates along with the boundary conditions Equations (13-15), is based on Fourier Spectral method [28-30]. In this method, the stream function, vorticity and temperature are approximated as a Fourier series expansion. This approach is related to that used by Mahfouz and Imtiaz [1], Collins and Dennis [28], Badr and Dennis [29] and Mahfouz and Badr [30]. The dimensionless stream function, vorticity and temperature are approximated using Fourier series expansions as follows:

$$\xi = \sum_{n=1}^{N} g_n \sin(n\theta) \tag{16}$$

$$\psi = \sum_{n=1}^{N} f_n \sin(n\theta) \tag{17}$$

$$\phi = \frac{H_o}{2} \sum_{n=1}^{N} H_n \cos(n\theta) \tag{18}$$

f_n, g_n, H_o and H_n are the Fourier coefficients and Equations (9-12) are replaced by their respective Fourier coefficients. The resulting equations (after multiplication at a time by 1, sin(nθ), cos(nθ)) are integrated with respect to θ between limits 0 and 2π. These equations can be written as:

$$e^{2\xi}\frac{\partial g_n}{\partial t} = pr\left[\frac{\partial^2 g_n}{\partial \xi^2} - n^2 g_n\right] + S_{1n}\left(n = 1,2,...N\right) \quad (19)$$

$$e^{2\xi} g_n = \frac{\partial^2 f_n}{\partial \xi^2} - n^2 f_n \quad (20)$$

$$e^{2\xi}\frac{\partial}{\partial t}\begin{pmatrix} H_o \\ H_n \end{pmatrix} = \frac{\partial^2}{\partial \xi^2}\begin{pmatrix} H_o \\ H_n \end{pmatrix} - n^2\begin{pmatrix} 0 \\ H_n \end{pmatrix} + \begin{pmatrix} S_{2n} \\ S_{3n} \end{pmatrix} \quad (21)$$

$$e^{2\xi}\frac{\partial}{\partial t}\begin{pmatrix} H_o \\ H_n \end{pmatrix} = \frac{\alpha_s}{\alpha}\left[\frac{\partial^2}{\partial \xi^2}\begin{pmatrix} H_o \\ H_n \end{pmatrix} - n^2\begin{pmatrix} 0 \\ H_n \end{pmatrix}\right] \quad (22)$$

Where S_{1n}, S_{2n} and S_{3n} are all easily identifiable functions of ξ and t. The boundary conditions in term of Fourier coefficients can be expressed as:

$$\text{At } \xi = \xi_i : H_o = 2, H_n = 0 \text{ for CWT while } \frac{\partial H_o}{\partial \xi} = -\frac{2}{Kr}, \frac{\partial H_n}{\partial \xi} = 0 \text{ for CHF} \quad (23)$$

$$\text{At } \xi = \xi_{sf} : \; k_s \frac{\partial H_o}{\partial \xi}\bigg|_{solid} = k_f \frac{\partial H_n}{\partial \xi}\bigg|_{fluid}, k_s \frac{\partial H_o}{\partial \xi}\bigg|_{solid} = k_f \frac{\partial H_o}{\partial \xi}\bigg|_{fluid} \quad (24)$$

$$\text{At } \xi = \xi_o : H_n = H_o = f_n = \frac{\partial f_n}{\partial \xi} = 0 \quad (25)$$

Equation (20) is multiplied by $e^{-n\xi}$ and then integrated with respect to ξ from $\xi = \xi_{sf}$ to $\xi = \xi_o$. After using Equation (24), the resulting equation can be written as:

$$\int_{\xi_{sf}}^{\xi_o} e^{(2-n)\xi} g_n d\xi = 0 \quad (26)$$

Equation (26) is used for calculating the g_n on the fluid side of the inner wall while g_n at outer wall can be calculated by using Equation (20) directly. Finite difference method is used for discretization of differential Equations (19-25) where all spatial derivatives are computed using central finite difference scheme. The first derivative on inner side of inner wall and at outer wall is approximated by second order accurate forward and backward three point finite difference scheme respectively. Equations (19, 21-22) are parabolic in time and are solved using Crank Nicolson scheme.

The numerical solution starts with eight terms only in the Fourier series and one more term is added when the last term exceeds the specified tolerance. The maximum number of terms depends on the Rayleigh number, heating method (CWT or CHF), radius radio and Kr. Upper limit for maximum number of Fourier terms is 35 for all cases considered in this work. The resulting coupled nonlinear system of equations has been linearized through an iterative procedure at each time step and has been solved by TDMA (Tri-Diagonal Matrix Algorithm). More details about solution procedure are given by Badr and Dennis [29] and Mahfouz and Badr [30].

2.4 Heat Transfer Parameters

The local Nusselt Number at the inner side of inner wall and at the solid-fluid interface is defined as:

$$Nu_i = \frac{q_i\left(2r_i\right)}{k_f \Delta T_{ref}}, Nu_{sf} = \frac{q_{sf}\left(2r_{sf}\right)}{k_f \Delta T_{ref}} \quad (27)$$

Where

$$q_i = -k_s\left(\frac{\partial T}{\partial S_n}\right)_i, q_{sf} = -k_f\left(\frac{\partial T}{\partial S_n}\right)_{sf}$$

Similarly the local Nusselt number at the outer wall is defined as:

$$Nu_o = \frac{q_o(2r_o)}{k_f \Delta T_{ref}}, q_o = -k_f \left(\frac{\partial T}{\partial S_n} \right)_o \quad (28)$$

The equivalent thermal conductivity along inner and outer wall is defined as:

$$K_{eq} = \frac{Nu}{Nu_{cond}} \quad (29)$$

Where Nu is the local Nusselt number either for inner or outer wall of the concentric annulus in case of zero thickness of inner wall. Moreover, Nu_{cond} is the Nusselt number when heat transfer through concentric annulus occurs only due to the conduction mode of heat transfer and it depends upon radius ratio i.e. $Nu_{cond} = 2/\ln Rr$.

The average Nusselt number can be seen as a dimensionless heat transfer rate at the wall and can be defined as:

$$\overline{Nu} = \frac{1}{2\pi} \int_0^{2\pi} Nu d\theta \quad (30)$$

In terms of Fourier coefficients, the average Nusselt number at the two sides of inner wall can be written as:

$$\overline{Nu_i} = -Kr \left(\frac{\partial H_o}{\partial \xi} \right)_i, \overline{Nu_{sf}} = -\left(\frac{\partial H_o}{\partial \xi} \right)_{sf}$$

And at the outer wall as:

$$\overline{Nu_o} = -\left(\frac{\partial H_o}{\partial \xi} \right)_o \quad (31)$$

The $\overline{Nu}$ calculated from Equation (30) is used to quantify the heat transfer rate through the concentric annulus. At the steady state, the energy conservation entails that $\overline{Nu}$ at heating side of inner wall would be equal to that of fluid side and both become equal to that of outer wall. That is, at the steady state the $\overline{Nu_i} = \overline{Nu_{sf}} = \overline{Nu_o}$.

In case of heating at CHF, the rate of heat transfer is known (heat flux multiplied by surface area) and for this case the most important parameter is the inner wall temperature which should be controlled in order to avoid the overheating of the annulus for industrial purposes. The value of ϕ for either side of the inner wall is calculated from Equation (18) and the corresponding mean dimensionless temperature is then calculated as:

$$\bar{\phi} = \frac{1}{2\pi} \int_0^{2\pi} \phi d\theta \quad (32)$$

3. RESULTS AND DISCUSSION

The governing equations along with the boundary conditions for both heating cases (CWT and CHF) are solved in order to give the details of both flow and thermal fields. The influencing parameters on conjugate heat transfer in the annulus are Rayleigh number Ra, Prandtl number Pr, radius ratio Rr($=r_o/r_i$), thickness of the solid wall given by Rs($=r_{sf}/r_i$) and the thermal conductivity of solid wall relative to that of fluid Kr ($= k_s/k_f$). This study considers Ra up to 10^5, a range of Rs from 1.0-3.0, a range of Kr from 0.25-100 and a range of Rr from 2-10. Pr is fixed at 0.7 for all cases except for the qualitative validation in case of CHF (Pr is taken as 0.01).

Before producing the numerical results, the validity of mathematical model and numerical technique has been first assessed by comparing the present results with the previous reliable results for the cases of CWT and CHF. The available results for both heating cases are only associated with horizontal concentric annulus having zero thickness of inner wall. The most pertinent previous work for CWT heating is that carried out by Kuehn and Goldstein [3]. Fig. 2 shows the qualitative comparison for streamlines and isotherms in CWT case and it shows that good agreement is achieved. Similarly, Fig. 3 shows quantitative comparison for K_{eq} with the experimental results of Kuehn and Goldstein [3] in CWT case and again a good agreement

is obtained. In order to verify the numerical model for CHF heating, a comparison with the work of Yoo [24] is made and the results of streamlines and isotherms are shown in Fig. 4. The figure shows that the present results are in good qualitative agreement with the numerical results of Yoo [24]. The quantitative comparison for CHF case is done with numerical results of Ho et. al. [26]. Fig. 5 shows good agreement between the present results and the numerical results of Reference [26].

In the following sections, the results that show the effect of controlling parameters on fluid flow and heat transfer characteristics for both heating cases (CHF & CWT) are presented. Section 3.1 considers the case of CWT while section 3.2 considers the case of CHF.

3.1 Heating at CWT

In case of heating at CWT the main target is to study the effect of controlling parameters on heat transfer rate exchanged through the annulus. The steady state heat transfer rate through the annulus depends on the overall thermal resistance between the two cylinders. This thermal resistance can be treated analogously as two electrical resistances in series. The first resistance is the conductive resistance due to solid wall of inner cylinder while the combined effect of conduction and free convection within fluid in the annulus can be considered as the second resistance. The conduction resistance depends on the thickness of conductive space and its thermal conductivity where it increases with the increase of the former and decreases with the increase of the latter. The convection resistance mainly depends on Ra and the space of the annulus. It decreases as Ra increases and

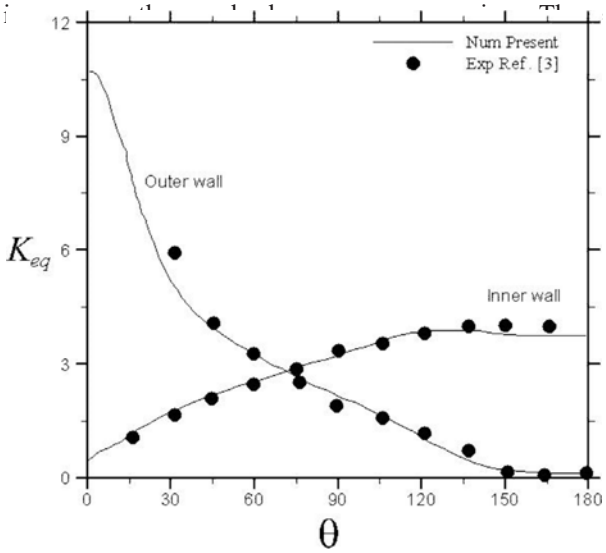

FIG. 3. STEADY EQUIVALENT THERMAL CONDUCTIVITY DISTRIBUTION ALONG INNER AND OUTER WALLS OF THE ANNULUS AND COMPARISON WITH [3] EXPERIMENTAL RESULTS FOR CWT CASE AT Ra_L = 5 X10⁴, Rr = 2.6, Rs = 1 AND Kr = 1

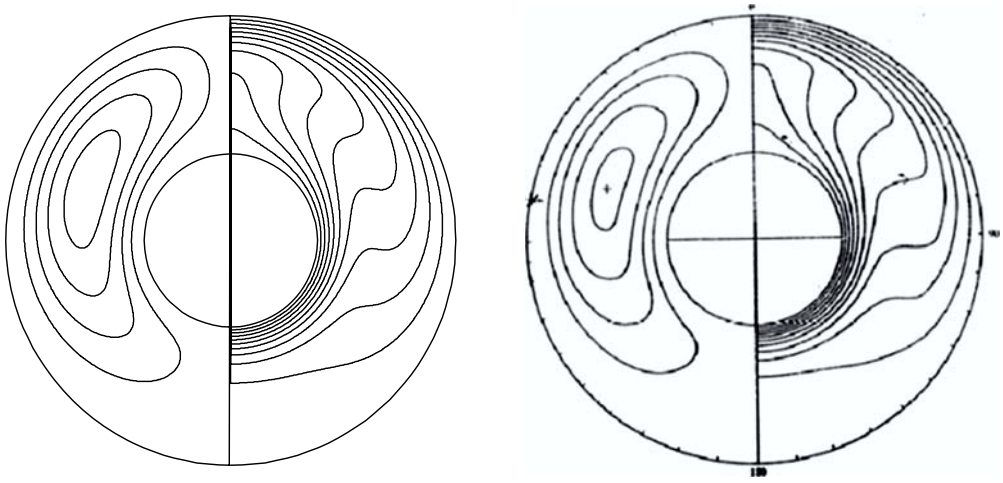

(a) *(b)*

FIG. 2. STEADY STREAMLINES (LEFT HALF) AND ISOTHERMS (RIGHT HALF) FOR CWT CASE AT Ra_L = 10⁴, Rr = 2.6, Rs = 1 AND Kr = 1 (a) PRESENT (b) REFERENCE [3]

conclusions are delineated through the following figures, tables and discussions.

The thickness of inner wall is a critical design parameter in high pressure systems such as nuclear reactor. Moreover, the variation of inner wall thickness impacts the heat transfer through the annulus. Fig. 6 shows the effect of inner wall thickness (represented by Rs) on the flow and thermal fields in the annulus. The figure shows the streamlines and isotherms at Ra = 10^4, Rr = 5, Pr = 0.7, Kr = 1.0 and at different values of Rs. It can be observed from the figure that the increase in Rs results in a reduction in the convection currents intensity as appears from the decrease of $|\psi|_{max}$ in the annulus. The reduction in convective flow intensity results in decrease in heat transfer rate (represented by $\overline{Nu}$) and causes less development of thermal plume in the upper part of the annulus.

In assembly of electronic components, the space is one of the major constraints so this work considers the effect of the two parameters that control the space of the annulus, these are Rr and Rs. Fig. 7 shows the flow and thermal fields at Ra = 10^4, Pr = 0.7, Rs = 1.3, Kr = 1.0 and at Rr = 2.0, 2.6, 5.0 and 10.0. While Fig. 6 shows the flow and thermal fields at Ra = 10^4, Pr = 0.7 Rr = 5, Kr = 1.0 and at Rs = 1.3, 1.5, 2.0 and 3.0. Figs. 6-7 show clearly that the increase in annulus space results in higher value of $|\psi|_{max}$ and heat transfer rate. The larger annulus space enhances the convection currents and in turn increases the rate of heat transfer.

Tables 1-2 represent the effect of Ra, Rr along with Rs on the steady state heat transfer rate through the annulus

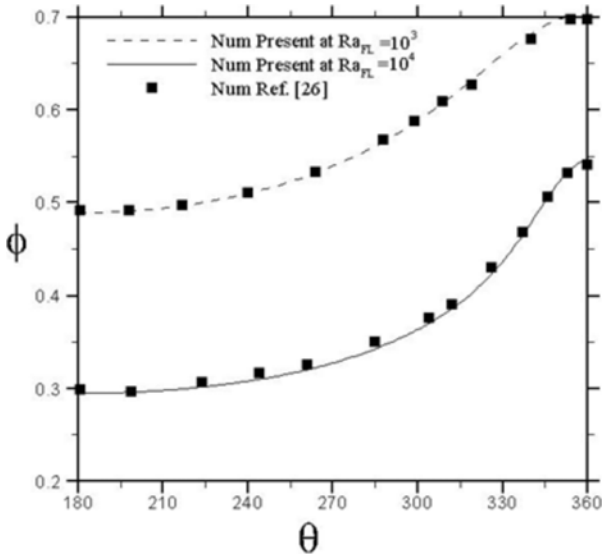

FIG. 5. DIMENSIONLESS INNER WALL TEMPERATURE AND COMPARISON WITH [26] RESULTS AT Rr = 2.6, Rs = 1.0 AND Kr = 1.0

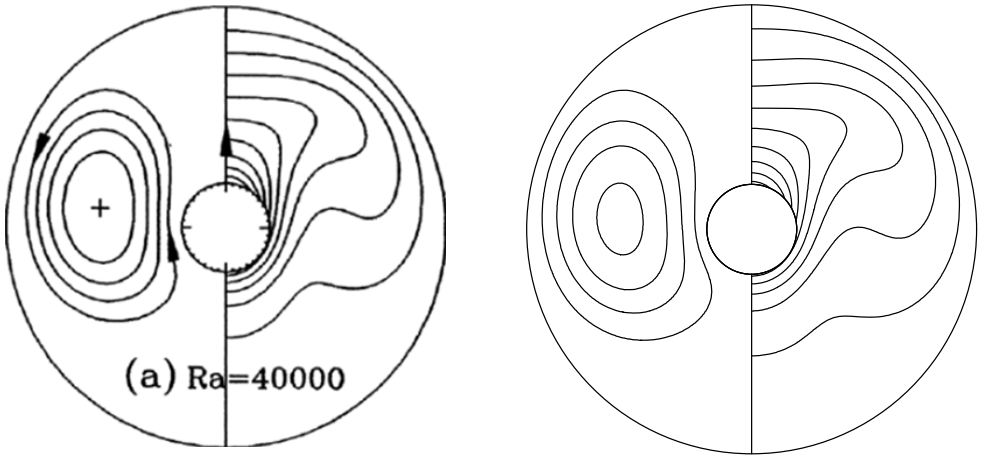

(a) *(b)*

FIG. 4. STEADY STREAMLINES (LEFT HALF) AND ISOTHERMS (RIGHT HALF) FOR THE CHF CASE OF Ra$_{FL}$ =4X10^4, Rr = 5.0, Rs = 1.0 AND Kr = 1.0 (a) PRESENT (b) REFERENCE [24]

(represented by $\overline{Nu}$) at Kr = 2.0 and Kr = 0.25, respectively. Pure conduction cases at Rr=2 are also shown in Tables 1-2. In Tables 1-2 two values of Ra are considered, the first is low (Ra = 10^3) and represents a conduction dominating case, while the second is relatively high (Ra = 10^5) and represents a convection dominating case. Quick inspection of the two tables confirms that for the same controlling parameters the increase of Ra and/or Kr increases the heat transfer rate through the annulus.

In conduction dominating case (Ra = 10^3), it can be noted from the two tables that the increasing Rr at fixed Rs causes decrease in heat transfer rate (i.e. $\overline{Nu}$), up to a certain value of Rr and then increases again with any further increase in Rr. The value of Rr at which heat transfer is minimum depends on the competence between the conductive and convective resistances, which are dependent on Ra, Kr and Rs as can be seen in Tables 1-2. The same thermal behavior can be observed for convection dominating flows (at Ra = 10^5) when annulus is narrow (at small Rr and bigger Rs). In case of wide annulus (at big Rr and small Rs) and high Ra the convection mode is dominating, causing the decrease in the overall thermal resistance and thus increasing heat transfer rate. It can also be observed that at small Rr = 2 and big Rs = 1.5, the values of $\overline{Nu}$ at Ra = 10^3 and Ra = 10^5 are very close to each other and very close to pure conduction value as well. This can be described by the fact that as the annulus space containing the fluid becomes extremely narrow, it eliminates the convective

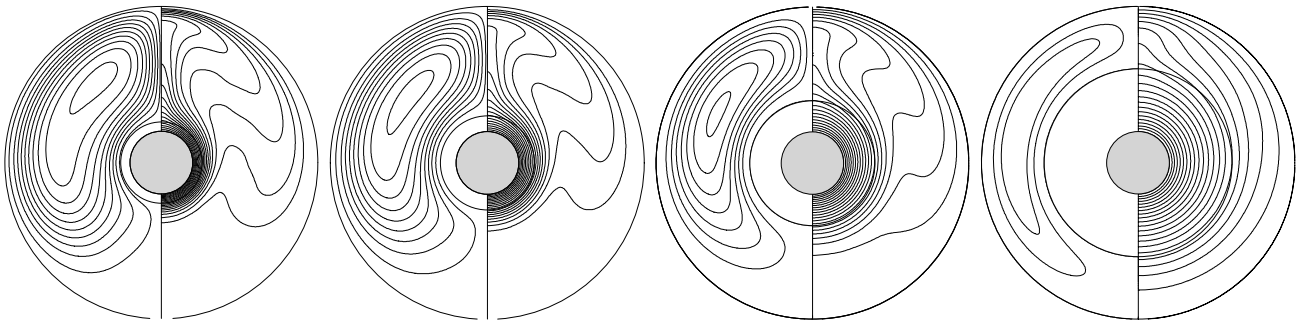

(a) (b) (c) (d)

FIG. 6.EFFECT OF Rs FOR CWT ON FLOW FIELDS (RIGHT SIDE IS STREAMLINES$\Delta\psi$=2 AND LEFT SIDE IS ISOTHERMS$\Delta\phi$ =0.05) AT Ra = 10^4, Rr = 5.0, Pr = 0.7. (a) Rs = 1.3, $|\psi|_{max} = 20$ & $\overline{Nu} = 3.087$ *(b) Rs = 1.5,* $|\psi|_{max} = 18$ & $\overline{Nu} = 2.371$ *(c) Rs = 2.0,* $|\psi|_{max} = 15$ & $\overline{Nu} = 1.814$ *(d) Rs = 3.0,* $|\psi|_{max} = 6$ & $\overline{Nu} = 1.336$

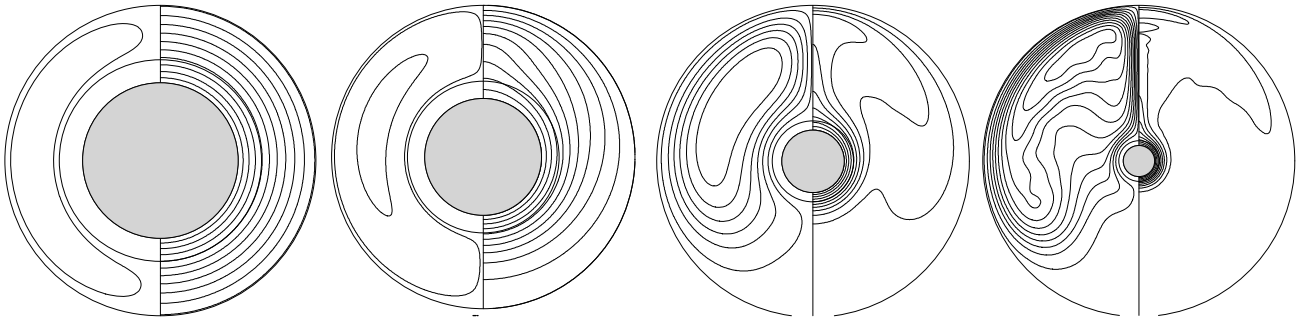

(A) (B) (C) (D)

FIG. 7. EFFECT OF Rr FOR CWT ON FLOW FIELDS (RIGHT SIDE IS STREAMLINES $\Delta\psi = 3.0$ *AND LEFT SIDE IS ISOTHERMS* $\Delta\phi = 0.1$*) AT Ra = 10^4, Rs = 1.3, Pr = 0.7. (a) Rr=2.0,* $|\psi|_{max} = 0.7$ & $\overline{Nu} = 2.890$ *(b) Rr=2.6,* $|\psi|_{max} = 4.4$ & $\overline{Nu} = 2.394$ *(c) Rr = 5.0,* $|\psi|_{max} = 19.0$ & $\overline{Nu} = 2.787$ *(d) Rr = 10.0,* $|\psi|_{max} = 34.0$ & $\overline{Nu} = 2.757$

mode of heat transfer. This explains the closeness of the to its two values at Ra = 10^3 and Ra =10^5 for pure conduction.

On the other side, for low conductivity inner wall material at Kr = 0.25 the increase in Rs means replacing the high conductive fluid at low Rayleigh number with lower conductive material, which in turn increases the overall thermal resistance and thus decreases the heat transfer through the annulus as can be seen in Table 2.

The thermal conductivity of material of inner wall plays a vital role in controlling heat transfer rate through the concentric annulus. In industrial applications, the replacement of Aluminum with Copper enhances the heat transfer through the annulus. In order to quantify the effect of Kr on heat transfer rates the results of steady $\overline{Nu}$ at Rs = 1.3 and at different values of Kr are presented in Table 3. It can be seen in Table 3 that as Kr increases from 0.5-100, the steady state $\overline{Nu}$ increases as a result of the decrease in overall thermal resistance. This increase

TABLE 1. EFFECT OF Ra, Rs AND Rr FOR CWT CASE ON $\overline{Nu}$ AT Kr = 2.0

Ra	Rr	$\overline{Nu}$			
		Rs = 1.2	Rs = 1.3	Rs = 1.4	Rs = 1.5
0	2.0	3.322	3.558	3.809	4.077
10^3	2.0	3.322	3.558	3.809	4.077
	2.6	2.328	2.433	2.543	2.657
	4.0	2.123	2.067	2.017	1.977
	5.0	2.347	2.286	2.229	2.174
10^5	2.0	4.538	4.154	3.995	4.112
	2.6	5.066	4.654	4.316	4.028
	4.0	5.271	4.862	4.531	4.259
	5.0	5.279	4.878	4.55251	4.284

TABLE 2 EFFECT OF Ra, Rs AND Rr FOR CWT CASE ON $\overline{Nu}$ AT Kr = 0.25

Ra	Rr	$\overline{Nu}$			
		Rs = 1.2	Rs = 1.3	Rs = 1.4	Rs = 1.5
0	2.0	1.613	1.351	1.175	1.047
10^3	2.0	1.613	1.351	1.175	1.047
	2.6	1.333	1.148	1.018	0.921
	4.0	1.199	1.002	0.875	0.788
	5.0	1.270	1.048	0.903	0.801
10^5	2.0	1.752	1.376	1.177	1.047
	2.6	1.835	1.407	1.157	0.993
	4.0	1.867	1.434	1.182	1.017
	5	1.867	1.434	1.184	1.019

is low in case of conduction dominating flows while for convection dominating flows, this increase is high. For instance, at Ra = 10^3, Rr = 5.0 the percentage increase in steady $\overline{Nu}$ is 81% as Kr = 0.5-100, whereas at Ra = 10^5, Rr = 5.0 this percentage goes to 217%.

3.2 Heating at CHF

This section focuses on the effect of controlling parameters on both flow and thermal fields in case of heating inner wall at CHF. In this case the inner wall temperature and temperature of the solid-fluid interface are the most important parameters for the annulus design. In case of heating at CWT, it was found that the steady state heat transfer rate through the annulus depends on the overall thermal resistance between the two cylinders. Similarly, in case of heating at CHF the dimensionless temperature of the two sides of the inner wall depends on the overall thermal resistance between the two cylinders. The overall thermal resistance dependence on the controlling parameters has been discussed in case of CWT. In case of CHF the smaller the thermal resistance, the higher the overall heat transfer coefficient is and thus the lower the temperature of the inner wall and vice versa.

Fig. 8 shows the streamlines and isotherms at $Ra_F = 10^4$, Rr = 5, Pr = 0.7, Kr = 1.0 and at different values for the thickness of inner wall which varies from Rs = 1.3 to Rs = 3. It can be noted (from the figure caption) that the increase in thickness (i.e. increase of Rs) results in rise of local maximum dimensionless temperature at inner wall. It can also be inferred that the reduction in the annulus space reduces the convection current intensity as can be observed from $|\psi|_{max}$. The effect of Rs on dimensionless stream function is similar to that for CWT as can be seen in Fig. 6. The effect of Rr on flow and thermal fields is shown in Fig. 9. The figure is plotted for the case of $Ra_F = 10^4$, Rs = 1.3, Pr = 0.7 at four values of Rr = 2.0, 2.6, 5.0 and 10.0. Fig. 7 shows that the increase in Rr increases the convection current intensity through the annulus and the same results were observed for CWT case.

Tables 4-5 present the effect of controlling parameters Ra_F, Rs and Rr on the steady state dimensionless temperature on the two sides of the inner wall at Kr = 2.0 and Kr = 0.25, respectively. The two tables have considered two values of Ra, (Ra = 10^3 and Ra = 10^5). The quick inspection of these tables shows that for the same controlling parameters the increase in Ra_F and/or Kr decreases the dimensionless average temperature of the two sides of the inner wall. It is needless to say that the

TABLE 3. EFFECT OF Ra, Kr AND Rr FOR CWT CASE ON $\overline{Nu}$ AT Rs=1.3

Ra	Rr	$\overline{Nu}$			
		Kr = 0.5	Kr = 1.5	Kr = 10	Kr = 100
10^3	2.0	2.093	3.302	4.376	4.614
	2.6	1.644	2.310	2.791	2.886
	4.0	1.414	1.966	2.352	2.426
	5.0	1.513	2.164	2.646	2.741
10^5	2.0	2.205	3.778	5.435	5.834
	2.6	2.323	4.182	6.371	6.923
	4.0	2.381	4.347	6.820	7.500
	5.0	2.383	4.359	6.862	7.556

temperature at the fluid side of the inner wall is less than that of the heating side. The temperature difference between heating side and fluid side depends on the inner wall thickness (Rs) and thermal conductivity ratio (Kr), the less Rs and/or the higher Kr, the smaller the temperature difference between the two inner wall sides. It can be observed from the two tables that the increase in Rs for conduction dominating cases ($Ra = 10^3$) leads to increase in inner wall temperature for $Kr < 1$, while at $Kr > 1$ the inner wall temperature rises with increase in Rs only at high Rr (i.e. $Rr \geq 2.6$). The effect of increase in Rs for convection dominating cases ($Ra_F = 10^5$) in the annulus results in an increase in inner wall temperature except for very narrow annulus space ($Rr = 2.0$) and $Kr > 1$.

Tables 4-5 also show the effect of Rr at fixed Rs on the inner wall dimensionless temperature where it can be seen for conduction dominating case that the increase in Rr at fixed Rs causes increase in inner wall temperatures till a certain value of Rr and then decreases again ($\overline{\phi_i}$, $\overline{\phi_{sf}}$) as Rr increases. The value of Rr at which ($\overline{\phi_i}$, $\overline{\phi_{sf}}$) is maximum depends on the competence between the conductive and convective resistances, which in turn are dependent on Ra_F, Kr and Rs as can be seen in the two tables. The same thermal behavior can be observed in convection dominating case (at $Ra_F = 10^5$) but only for narrow annulus (at bigger Rs).

The material properties of inner wall for CHF heating are investigated in Table 6, which shows the effect of Kr on inner wall temperature of concentric annulus. It shows that increase in Kr (from 0.5 to 100) reduces the inner wall dimensionless temperature at constant Rr and Ra_F. This

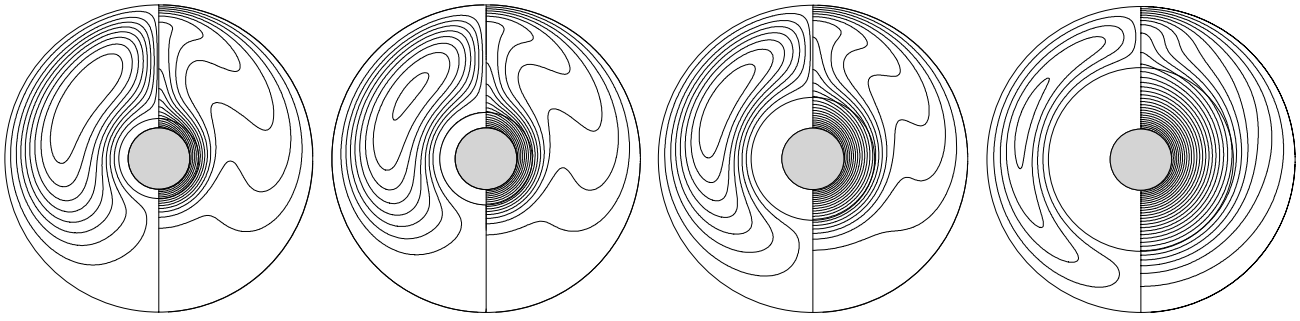

(a) *(b)* *(c)* *(d)*

FIG. 8. EFFECT OF Rs FOR CHF ON FLOW FIELDS (RIGHT SIDE IS STREAMLINES $\Delta\psi = 2$ AND LEFT SIDE IS ISOTHERMS $\Delta\phi = 0.05$) AT $Ra_F = 10^4$, Rr = 5, Pr = 0.7 (a) Rs = 1.3, $|\psi|_{max} = 17$ & $\phi_{max} = 0.95$ (b) Rs = 1.5, $|\psi|_{max} = 17$ & $\phi_{max} = 1.05$ (c) Rs = 2.0, $|\psi|_{max} = 15$ & $\phi_{max} = 1.25$ (d) Rs = 3.0, $|\psi|_{max} = 8$ & $\phi_{max} = 1.60$

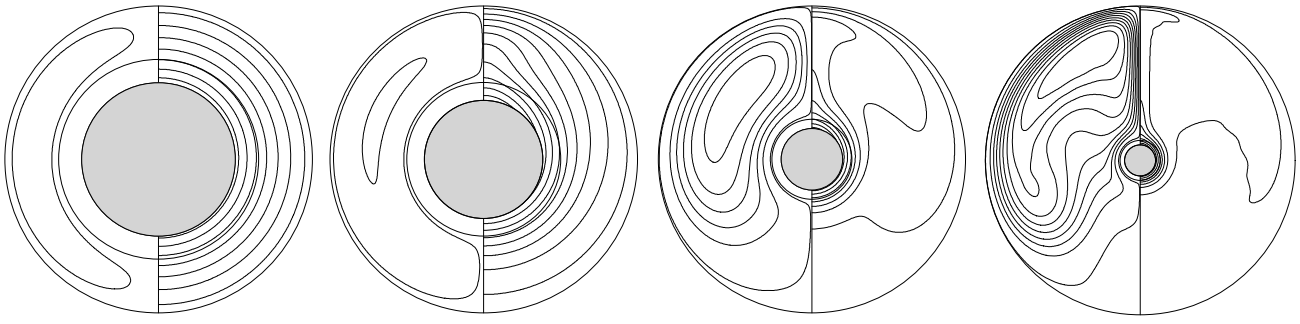

(a) *(b)* *(c)* *(d)*

FIG. 9. EFFECT OF Rr FOR CHF ON FLOW FIELDS (RIGHT SIDE IS STREAMLINES $\Delta\psi = 3.0$ AND LEFT SIDE IS ISOTHERMS $\Delta\phi = 0.1$) AT $Ra_F = 10^4$, Rs = 1.3, Pr = 0.7 (a) Rr = 2.0, $|\psi|_{max} = 0.5$ & $\phi_{max} = 0.75$ (b) Rr = 2.6, $|\psi|_{max} = 3.6$ & $\phi_{max} = 1.05$ (c) Rr = 5.0, $|\psi|_{max} = 17.0$ & $\phi_{max} = 0.95$ (d) Rr = 10.0, $|\psi|_{max} = 30.0$ & $\phi_{max} = 0.90$

decrease is attributed to increase in thermal conductivity of inner wall. At low Rayleigh number (i.e. $Ra_F = 10^3$), Rr = 5.0 the percentage decrease in steady $\overline{\phi_i}$ is 40% as Kr increases from 0.5-100, while at high Rayleigh number (i.e. $Ra_F = 10^5$), Rr = 5.0 the percentage decrease in steady $\overline{\phi_i}$ goes to 61%. It can be inferred from these results that the effect of Kr is more significant in case of convective dominating cases as can be seen in Table 6.

One further observation that can be inferred from data of Table 6 is that the effect of increase in Kr on steady $\overline{\phi_i}$ not only depends on Ra but also on Rr. For conduction dominating case (i.e. $Ra_F = 10^3$), the percentage decrease in steady $\overline{\phi_i}$ is 55% as Kr = 0.5 to 100 at Rr = 2.0 while at Rr = 5.0 this percentage decrease in steady $\overline{\phi_i}$ goes to 40%. It can be noted that effectiveness of increase in Kr on percentage decrease in steady $\overline{\phi_i}$ reduces as Rr changes from 2.0-5.0 for conduction dominating case. For convective flows (i.e. $Ra_F = 10^5$), the percentage decrease in steady $\overline{\phi_i}$ is 57% as Kr increases from 0.5-100 at Rr = 2.0, whereas at Rr = 5.0 the percentage decrease in steady $\overline{\phi_i}$ goes to 61%. It shows that effectiveness of increasing Kr on percentage decrease in steady increases as Rr changes from 2.0-5.0 for convection dominating flows.

TABLE 4. EFFECT OF Ra_F, Rs AND Rr ON $\overline{\phi_i}$ AND $\overline{\phi_{sf}}$ FOR CHF CASEAT Kr = 2.0

Ra_F	Rr	Rs = 1.2		Rs = 1.3		Rs = 1.4		Rs = 1.5	
		$\overline{\phi_i}$	$\overline{\phi_{sf}}$	$\overline{\phi_i}$	$\overline{\phi_{sf}}$	$\overline{\phi_i}$	$\overline{\phi_{sf}}$	$\overline{\phi_i}$	$\overline{\phi_{sf}}$
10^3	2	0.583	0.493	0.561	0.430	0.525	0.357	0.490	0.288
	2.6	0.857	0.766	0.820	0.689	0.786	0.617	0.752	0.549
	4	0.915	0.824	0.941	0.810	0.957	0.790	0.980	0.777
	5	0.842	0.751	0.864	0.733	0.886	0.718	0.907	0.704
10^5	2	0.419	0.328	0.517	0.386	0.514	0.346	0.489	0.286
	2.6	0.439	0.348	0.477	0.346	0.507	0.339	0.539	0.337
	4	0.435	0.344	0.461	0.330	0.476	0.308	0.501	0.298
	5	0.419	0.328	0.446	0.315	0.472	0.304	0.497	0.294

TABLE 5. EFFECT OF Ra_F, Rs AND Rr ON $\overline{\phi_i}$ AND $\overline{\phi_{sf}}$ FOR CHF CASEAT Kr = 0.25

Ra_F	Rr	Rs = 1.2		Rs = 1.3		Rs = 1.4		Rs = 1.5	
		$\overline{\phi_i}$	$\overline{\phi_{sf}}$	$\overline{\phi_i}$	$\overline{\phi_{sf}}$	$\overline{\phi_i}$	$\overline{\phi_{sf}}$	$\overline{\phi_i}$	$\overline{\phi_{sf}}$
10^3	2	1.240	0.511	1.480	0.431	1.702	0.357	1.909	0.288
	2.6	1.495	0.765	1.739	0.690	1.964	0.618	2.171	0.549
	4	1.548	0.819	1.843	0.793	2.124	0.778	2.386	0.765
	5	1.477	0.747	1.777	0.728	2.056	0.710	2.317	0.696
10^5	2	1.121	0.391	1.429	0.379	1.691	0.345	1.908	0.286
	2.6	1.076	0.346	1.393	0.344	1.682	0.336	1.955	0.333
	4	1.072	0.343	1.367	0.318	1.652	0.307	1.919	0.297
	5	1.057	0.328	1.364	0.315	1.649	0.303	1.915	0.293

TABLE 5. EFFECT OF Ra_F, Kr AND Rr ON $\overline{\phi_i}$ AND $\overline{\phi_{sf}}$ FOR CHF CASEAT Rs = 1.3

Ra_F	Rr	Kr = 0.5		Kr = 1.5		Kr = 10		Kr = 100	
		$\overline{\phi_i}$	$\overline{\phi_{sf}}$	$\overline{\phi_i}$	$\overline{\phi_{sf}}$	$\overline{\phi_i}$	$\overline{\phi_{sf}}$	$\overline{\phi_i}$	$\overline{\phi_{sf}}$
10^3	2	0.955	0.431	0.606	0.431	0.457	0.430	0.427	0.425
	2.6	1.215	0.690	0.865	0.690	0.712	0.686	0.670	0.667
	4	1.319	0.795	0.974	0.800	0.850	0.824	0.830	0.828
	5	1.253	0.729	0.907	0.732	0.775	0.749	0.753	0.751
10^5	2	0.904	0.377	0.560	0.385	0.418	0.392	0.384	0.381
	2.6	0.869	0.344	0.520	0.345	0.379	0.353	0.354	0.351
	4	0.842	0.318	0.493	0.318	0.359	0.333	0.325	0.323
	5	0.839	0.315	0.490	0.315	0.344	0.318	0.325	0.323

4. CONCLUSIONS

In this paper, the problem of conjugate heat transfer within a concentric annulus filled with Newtonian fluid is numerically investigated using Fourier Spectral method. The inner wall of annulus is heated either through isothermal heating (CWT) or CHF, while the outer wall is cooled and kept at constant low temperature. The study focuses on the CHF along CWT, as CHF has significant role in high pressure industrial applications but has not received much attention. The conjugate heat transfer in the annulus depends on radius ratio Rr, thermal conductivity ratio Kr, and thickness of inner wall Rs. This study considers Rayleigh number up to 10^5, a range of Rs from 1.2-3.0, a range of Kr from 0.25-100 and range of Rr from 2-10. The Pr is fixed at 0.7 except for validation study of CHF heating. The study has shown that as Rayleigh number increases the heat transfer rate through the annulus increases for CWT heating, while the inner wall dimensionless temperature decreases for CHF heating. The study has also shown that the increase in Kr increases the heat transfer through annulus for CWT heating and decreases the inner wall dimensionless temperature for CHF heating and vice versa. It has also been proved that as the inner wall thickness increases at fixed Rayleigh number and Rr, the heat transfer rate decreases for CWT heating and the inner wall dimensionless temperature increases for CHF heating at Kr <1. The study has also discussed that at Kr>1, the effect of increase in Rs either on heat transfer for CWT heating or inner wall dimensionless temperature for CHF heating also depends on Rr. It has been shown for certain combinations of controlling parameters there is a value of Rr at which heat transfer rate is minimum in the annulus in case of CWT heating, while there is a value of Rr at which dimensionless temperature is maximum in the annulus in case of CHF. Moreover, the study has concluded that the effectiveness of increase in Kr is more at high Rayleigh numbers for both heating cases (CHF or CWT).

5. NOMENCLATURE

f_n	Fourier coefficients
F_r,F_θ	radial and tangential components of buoyancy force
g	gravitational acceleration
g_n	Fourier coefficient
H_o,H_n	Fourier coefficients
K_{eq}	equivalent thermal conductivity
k_f	thermal conductivity of fluid
Kr	thermal conductivity ratio ($= k_s/k_f$)

k_s	thermal conductivity of inner wall
L	difference of radius $=r_o-r_i$
Nu,	local and average Nusselt numbers
Nu_{cond}	Conduction Nusselt number (= 2/ln Rr)
Pr	Prandtl number ($\mu/\rho\alpha$)
R	dimensionless radial coordinate (r/r_i)
Ra	Rayleigh number based on ($2r_i$) for CWT case
Ra_F	modified Rayleigh number based on (2) for CHF case
Ra_L	Rayleigh number based on ($L=r_o-r_i$) for CWT case
Ra_{FL}	modified Rayleigh number based on ($L=r_o-r_i$) for CHF case
r_i	radius of inner side of inner wall
r_o	radius of outer wall
Rr	radius ratio ($=r_o/r_i$)
r_{sf}	radius of the fluid side of inner wall
R_s	dimensionless radius at the interface ($= r_{sf}/r_i$)
R_o	dimensionless radius at the outer wall ($= r_o/r_i$)
q_i	uniform heat flux applied on heating side of inner wall
t	dimensionless time
T	temperature
$\bar{x}, \bar{y}$	dimensionless Cartesian coordinates (x/r_i, y/r_i)

Greek Symbols

α	thermal diffusivity
β	coefficient of thermal expansion
ΔT_{ref}	temperature difference = T_o-T_i in case of CWT and equal to r_iq_i/k in case of CHF
ϕ	dimensionless temperature $(T-T_i)/\Delta T_{ref}$
ξ	dimensionless logarithmic coordinate (= ln R)
μ	dynamic viscosity.
ν	kinematics viscosity
ρ	density
τ	time
θ	angular coordinate
ψ', ψ	stream function and dimensionless stream function
ζ', ζ	vorticity and dimensionless vorticity

Subscripts

i	at inner side of inner wall
sf	at solid-fluid interface
o	at outer wall of the annulus

ACKNOWLEDGEMENTS

The support received from Menoufia University, Egypt, and National University of Sciences & Technology, Islamabd, Pakistan, is highly appreciated. The first author would also like to thank Umber Saleem, Post-Graduate Student, Department of Electrical Engineering, National University of Sciences & Technology, Pakistan, for correcting the grammatical errors.

REFERENCES

[1] Mahfouz, F.M., and Imtiaz, H., "Free Convection within an Eccentric Annulus Filled with Micropolar Fluid", Proceedings of 9th International Bhurban Conference on Applied Sciences & Technology, Islamabad, Pakistan, pp. 308–317, 2012.

[2] Mahfouz, F.M., "Numerical Prediction of Buoyancy Driven Micropolar Fluid Flow within Uniformly Heated Eccentric Annulus", Applied Mathematical Modeling, Volume 37, pp. 6037–6054, 2013.

[3] Kuehn, H., and Goldstein, R.J., "An Experimental and Theoretical Study of Natural Convection in the Annulus between Horizontal Concentric Cylinders", Journal of Fluid Mechanics, Volume 74, pp. 695-719, 1976.

[4] Imtiaz, H., and Mahfouz, F.M., "Conjugate Heat Transfer within a Concentric Annulus Filled with Micropolar Fluid", Journal of Heat and Mass Transfer, Volume 50, No. 4, pp. 457-468, 2013,

[5] Mahfouz, F.M., "Heat Convection within an Eccentric Annulus Heated at either Constant Wall Temperature or Constant Heat Flux", ASME, Journal of Heat Transfer, Volume 134, No. 8, pp. 1-9, 2012.

[6] Abbott, M.R., "A Numerical Method for Solving the Equations of Natural Convection in Narrow Concentric Cylindrical Annulus with a Horizontal Axis", The Quarterly Journal of Mechanics and Applied Mathematics, Volume 17, No. 4, pp. 471-481, 1964.

[7] Grigull, U., and Hauf, W., "Natural Convection in Horizontal Cylindrical Annuli", Proceeding of the 3rd International Heat Transfer Conference, Volume 2, pp. 182-195, 1966.

[8] Mack, L.R., and Bishop, E.H., "Natural Convection between Horizontal Concentric Cylinders for Low Rayleigh Numbers", The Quarterly Journal of Mechanics and Applied Mathematics, Volume 21, pp. 223-241, 1968.

[9] Kuehn, H., and Goldstein, R.J., "An Experimental Study of Natural Convection Heat Transfer in Concentric and Eccentric Horizontal Cylindrical Annuli", ASME, Journal of Heat Transfer, Volume 100, pp. 635–640, 1978.

[10] Walton, I.C., "The Stability of Free Convection in a Horizontal Cylindrical Annulus", The Quarterly Journal of Mechanics and Applied Mathematics, Volume 33, pp. 125-139, 1980.

[11] Farouk, B., and Güceri, S.I., "Laminar and Turbulent Natural Convection in the Annulus between Horizontal Concentric Cylinders", Journal of Heat Transfer, Volume 104, pp. 631-636, 1982.

[12] Tsui, Y.T., and Trembaly, B., "On Transient Natural Convection Heat Transfer in the Annulus between Concentric Horizontal Cylinders with Isothermal Surfaces", International Journal of Heat and Mass Transfer, Volume 27, No. 1, pp. 103-111, 1983.

[13] Mizushima, J., Hayashi, S., and Adachi, T., "Transitions of Natural Convection in a Horizontal Annulus", International Journal of Heat and Mass Transfer, Volume 44, pp. 1249-1257, 2001.

[14] ElSherbiny, S.M., and Moussa, A.R., "Effects of Prandtl Number on Natural Convection in Horizontal Annular Cavities", Alexandria Engineering Journal, Volume 43, pp. 561-576, 2004.

[15] Alshahrani, D., Zeitoun, O., "Natural Convection in Horizontal Cylindrical Annuli", Alexandria engineering Journal, Volume 44, pp. 813-823, 2005.

[16] Padilla, E.L.M., Campregher, R., and Silveira-Neto, A., "Numerical Analysis of the Natural Convection in Horizontal Annuli at Low and Moderate Ra", Engenharia Térmica (Thermal Engineering), Volume **5**, pp. 58-65, 2006.

[17] Hassan, A.K., and Al-lateef, J.M.A., "Numerical Simulation of Two Dimensional Transient Natural Convection Heat Transfer from Isothermal Horizontal Cylindrical", Journal of Engineering, Volume 13, No. 2, pp. 1429-1444, 2007.

[18] El-Sherbiny, S.M., and Moussa, A.R., "Natural Convection in Air Layers between Horizontal Concentric Isothermal Cylinders", Alexandria Engineering Journal, Volume 43, pp. 297-311, 2004.

[19] Ha, M.Y., and Kim, J.G., "Numerical Simulation of Natural Convection in Annuli with Internal Fins", KSME International Journal, Volume 18, No. 4, pp. 718-730, 2004.

[20] Oztop, H.F., Zhao, Z., and Bo, Y., "Fluid Flow due to Combined Convection in Lid-Driven Enclosure Having a Circular Body", International Journal of Heat and Fluid Flow, Volume 30, pp. 886–901, 2009.

[21] Oztop, H.F., and Abu-Nada, E., "Numerical Study of Natural Convection in Partially Heated Rectangular Enclosures Filled with Nanofluids", International Journal of Heat and Fluid Flow, Volume 29, No. 5, pp. 1326-1336, 2008.

[22] Kumar, R., "Study of Natural Convection in Horizontal Annuli", International Journal of Heat and Mass Transfer, Volume 31, No. 6, 1137–1148, 1988.

[23] Castrejon, A., and Spalding, D.B., "An Experimental and Theoretical Study of Transient Free-Convection Flow between Horizontal Concentric Cylinders", International Journal of Heat and Mass Transfer, Volume 31, No. 2, pp. 273–284, 1988.

[24] Yoo, J.S., "Flow Pattern Transition of Natural Convection in a Horizontal Annulus with Constant Heat Flux on the Inner Wall", International Journal of Numerical Methods for Heat & Fluid Flow, Volume 15, No. 7, pp. 698-709, 2004.

[25] Yoo, J.S., "Dual Free-Convective Flows in a Horizontal Annulus with a Constant Heat Flux Wall", International Journal of Heat and Mass Transfer, Volume 46, pp. 2499–2503, 2003.

[26] Ho, C.J., Lin, Y.H., and Chen, T.C., "A Numerical Study of Natural Convection in Concentric and Eccentric Horizontal Cylindrical Annuli with Mixed Boundary Conditions", International Journal Heat and Fluid Flow, Volume 10, No. 1, pp. 40-47, 1987.

[27] Kolesnikov, P.M., and Bubnovich, V.I., "Non-Stationary Conjugate Free-Convective Heat Transfer in Horizontal Cylindrical Coaxial Channels", International Journal of Heat and Mass Transfer, Volume 31, No. 6, pp. 1149-1155, 1988.

[28] Collins, W.M., and Dennis, S.C.R., "Flow Past an Impulsively Started Circular Cylinder", Journal of Fluid Mechanics, Volume 60, pp. 105-127, 1973.

[29] Badr, H.M., and Dennis, S.C.R., "Time-Dependent Viscous Flow Past an Impulsively Started Rotating and Translating Circular Cylinder", Journal of Fluid Mechanics, Volume 158, pp. 447-488, 1985.

[30] Mahfouz, F.M., and Badr, H.M., "Flow Structure in the Wake of a Rotationally Oscillating Cylinder", ASME, Journal of Fluids Engineering, Volume 122, pp. 290-301, 2000.